

A Study of Hygrothermal Behavior of ACF Flip Chip Packages With Moiré Interferometry

Jin-Hyoung Park, Kyung-Woon Jang, Kyung-Wook Paik, and Soon-Bok Lee

Abstract—A primary factor of anisotropic conductive film (ACF) package failure is delamination between the chip and the adhesive at the edge of the chip. This delamination is mainly affected by the thermal shear strain at the edge of the chip. This shear strain was measured on various electronic ACF package specimens by micro-Moiré interferometry with a phase shifting method. In order to find the effect of moisture, the reliability performance of an adhesive flip-chip in the moisture environment was investigated. The failure modes were found to be interfacial delamination and bump/pad opening which may eventually lead to total loss of electrical contact. Different geometric size specimens in terms of interconnections were discussed in the context of the significance of mismatch in coefficient of moisture expansion (CME) between the adhesive and other components in the package, which induces hygroscopic swelling stress. The effect of moisture diffusion in the package and the CME mismatch were also evaluated by using the Moiré interferometry. From Moiré measurement results, we could also obtain the stress intensity factor K . Through an analysis of deformations induced by thermal and moisture environments, a damage model for an adhesive flip-chip package is proposed.

Index Terms—Anisotropic conductive film (ACF), coefficient of moisture expansion (CME), delamination, electronic packaging, Moiré interferometry, reliability.

I. INTRODUCTION

FLIP-CHIP assemblies using an adhesive have been increasingly applied to personal digital assistant devices, mobile phones, and liquid crystal display devices. The use of adhesive flip-chip-type electronic packages offers numerous advantages such as reduced thickness, improved environmental compatibility, lowered costs, low process temperature, and fine pitch application, in addition to being a “green” technology [1], [2]. The use of anisotropic conductive film (ACF) for

Manuscript received November 12, 2008; revised April 28, 2009 and September 24, 2009. Current version published March 10, 2010. This work was supported by Grant N01080268 from the Center for Nanoscale Mechatronics and Manufacturing, one of the 21st Century Frontier Research Programs, which are supported by the Ministry of Education, Science, and Technology, Korea. Recommended for publication by Associate Editor X. Fan upon evaluation of reviewers’ comments.

J.-H. Park and S.-B. Lee are with the Department of Mechanical Engineering, Korea Advanced Institute of Science and Technology, Daejeon 305-701, Korea (e-mail: turbomb@kaist.ac.kr; sblee@kaist.ac.kr).

K.-W. Jang is with the Mechatronics and Manufacturing Technology Center, Samsung Electronics, Suwon 442-742, Korea (e-mail: k.w.jang@samsung.com).

K.-W. Paik is with the Department of Materials Science and Engineering, Korea Advanced Institute of Science and Technology, Daejeon 305-701, Korea (e-mail: kwpaik@kaist.ac.kr).

Color versions of one or more of the figures in this paper are available online at <http://ieeexplore.ieee.org>.

Digital Object Identifier 10.1109/TCAPT.2009.2036154

the direct interconnection of flipped silicon chips to printed circuits also offers numerous advantages such as reduced thickness, improved environmental compatibility, lowered assembly process temperature, increased metallization options, cut down costs, and decreased equipment requirements. Its wide application to glass displays through a chip on glass process has accelerated interest in using this technology on rigid/flexible substrates and even on paper substrates as novel ACFs are being developed.

ACF-type packages for flip-chip packages are becoming more popular among producers due to the simple processing involved, as well as the direct contact provided between the bump and electrode. Despite numerous benefits, flip-chip-type packages still suffer from several reliability problems. The most critical issue among them is electrical performance deterioration upon consecutive thermal cycle damage and moisture absorption of the polymeric resin. The latter is attributed to gradual delamination growth at the chip and adhesive film interface induced by coefficient of thermal expansion (CTE) and coefficient of moisture expansion (CME) mismatch driven shear and peel stresses. When a crack at a weak site of the electronic package forms, thermal and swelling deformation of the flip-chip package occurs.

In recent years, the Moiré method has been used extensively in the electronics industry to determine thermal strains caused by temperature changes in microelectronics devices such as ACF packages [3]–[6]. In particular, the Moiré interferometry method, which utilizes a diffraction grating and interference of laser beams [7], is used in this paper.

In this paper, microdeformations of ACF packages are measured by Moiré interferometry [8]–[10]. Optical methods are used for the measurement of the thermal and swelling deformations. Twyman–Green interferometry is applied to measure the out-of-plane deformations. Through the Twyman–Green experiment, it is possible to obtain the thermal warpage of the ACF chip [11], [12]. Moiré interferometry is applied to measure the in-plane deformations of ACF packages.

The CME mismatch between ACF and other components induces hygroscopic swelling stress. A fully moistured ACF specimen and a dried specimen are evaluated in order to calculate the interfacial fracture toughness from Moiré experiments.

II. SPECIMENS

In this paper, the hygrothermal behavior of an ACF-type package was evaluated (Fig. 1). A conventional ACF using



Fig. 1. ACF package specimens.

TABLE I
ACF PACKAGE SPECIMENS

Specimen	Thickness of Chip (μm)	Thickness of PCB (μm)	Fillet*	Life (cycles)
S1	180	120	×	14 223
S2	180	550	×	15 121
S3	180	980	×	4687
S4	480	120	×	11 743
S5	480	550	×	11 744
S6	480	980	×	2737
NF	780	980	×	2533
WF	780	980	o	4665

NF: specimen without fillet; WF: specimen with fillet.

* (×) Without fillet. (o) With fillet.

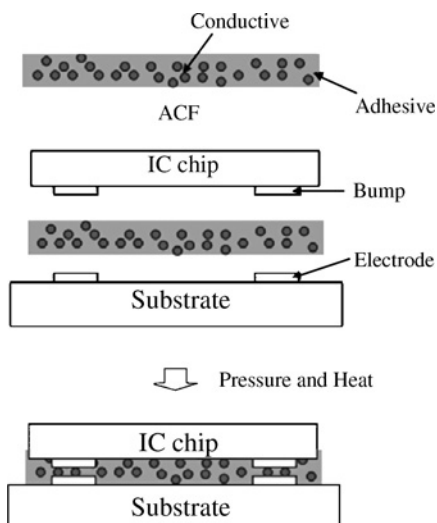


Fig. 2. Bonding procedure for flip-chip using ACF.

di-functional epoxies is used for this paper. This ACF has a general polymer matrix and a glass transition temperature of 108°C . In order to observe the effect of the different geometric shape, the following ACF specimens have been used (Table I).

The bonding conditions for all specimens were equal at 45 MPa and 180°C for 20s (Fig. 2). The geometric size of all specimens was not varied, except the thicknesses of the chip and printed circuit board (PCB). The thickness of the ACF was $50\ \mu\text{m}$, and the dimensions of the chip were $8\ \text{mm} \times 8\ \text{mm}$. The dimensions of the gold bumps in the chip plate were $120\ \mu\text{m} \times 120\ \mu\text{m} \times 18\ \mu\text{m}$, and the pitches of the peripheral bumps were all $130\ \mu\text{m}$. The size of the PCB was $20\ \text{mm} \times 20\ \text{mm}$.

In order to observe the effect of the fillet at the edge of the chip, the following other ACF specimens were also used (Table I). The geometric size of all specimens was also equal. The thickness of the ACF was $50\ \mu\text{m}$, and the dimensions of the chip were $8\ \text{mm} \times 8\ \text{mm}$. The dimensions of the gold bumps in the chip plate were $120\ \mu\text{m} \times 120\ \mu\text{m} \times 18\ \mu\text{m}$,

TABLE II
MATERIAL PROPERTIES

	Modulus (GPa)	CTE (ppm/ $^\circ\text{C}$)	ν	T_g ($^\circ\text{C}$)
Die	170	2.45	0.28	—
ACF	2.4 (under T_g)	$a_1 = 46$ $a_2 = 158$	0.34	108
Substrate	17.2	$\alpha_x = \alpha_y = 20$ $\alpha_z = 50$	0.15	180

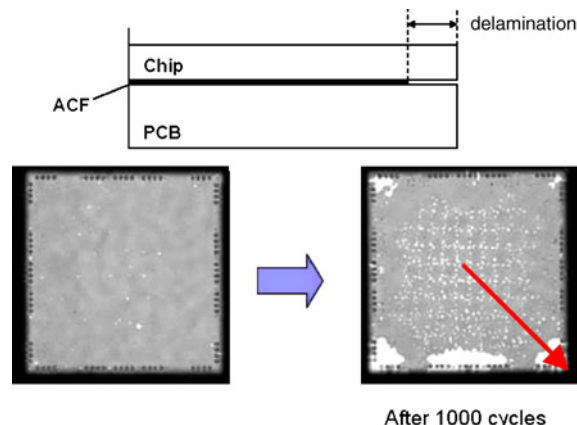


Fig. 3. Delamination of ACF specimen.

and the pitches of the peripheral bumps were all $130\ \mu\text{m}$. The size of the PCB was $20\ \text{mm} \times 20\ \text{mm}$. The properties of each material are listed in Table II [13].

III. THERMAL TESTS

Temperature cycling tests of the ACF-type specimens were performed in a thermal chamber. Thermal cycling was performed in a temperature range of $(-40^\circ\text{C}$ to 150°C . The holding time of upper and lower was 10 min. The resistance value was measured at 24 points for each specimen simultaneously during temperature cycling tests. The failure was determined when the resistance reaches to $220\ \text{m}\Omega$. The failure modes were found to be interfacial delamination and bump/pad opening, which may eventually lead to the total loss of electrical contact (Fig. 3). The thermal fatigue life in this paper was the average value of four specimens (Table I).

The bonding of ACF-type specimens is conducted at high temperature. Therefore, the ACF-type specimens at room temperature show a bent shape due to CTE mismatch of each material. Twyman–Green interferometry was applied to measure the bending deformation. Through the experiment with Twyman–Green interferometry, warpage of the ACF chip site was determined. This optical system can measure the global warpage behavior in a die chip. The resolution of the Twyman–Green interferometry was the half of the wavelength of the laser light source, i.e., $\lambda/2 = 0.316\ \mu\text{m}/\text{fringe}$ [14]–[16]. The out-of-plane deformations in the chip were measured at room temperature. It was found that the ACF package provides a stress-free condition at the temperature above T_g . The warpage results at room temperature are shown in Fig. 4. Generally, thin die chips showed large warpage, but the warpage value was not strongly related to the thermal fatigue life (Fig. 5). The very large warpage may lead to the delamination of the

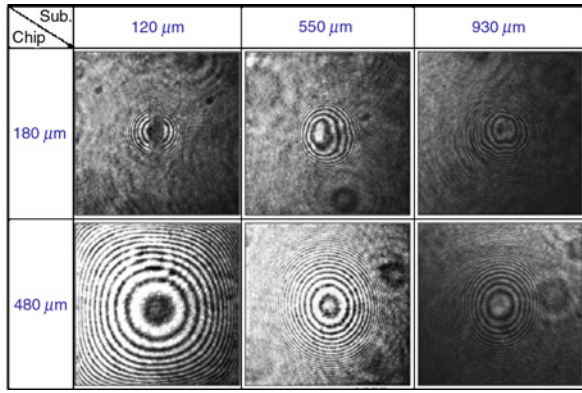


Fig. 4. Warpage of ACF-type specimens at room temperature.

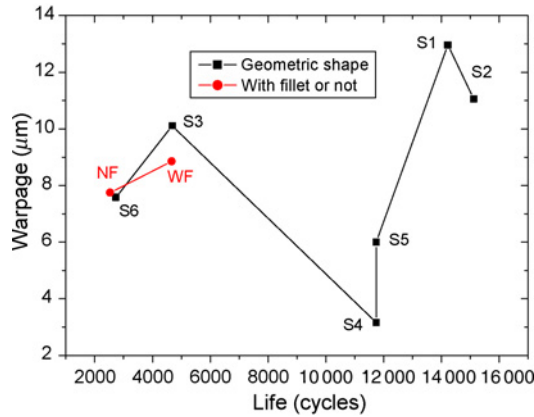


Fig. 5. Relations between thermal life and warpage.

interconnection layer. The moderate warpage value does not affect the thermal fatigue life. Therefore, the warpage value is not a good thermal fatigue damage parameter.

The main fracture mechanism during thermal cycles is delamination between the chip and ACF. This delamination occurs mainly by a shear strain at the edge of the chip. Therefore, precise evaluation of the shear strain is important for prediction of ACF-type package lifetime.

The in-plane measurement results from the investigation of the shear strain at the edge of the chip are shown in Fig. 6. In the measurements by Twyman–Green interferometry, ACF-type specimens showed a zero warpage above T_g of 108 °C, which means a stress-free condition. Since above 108 °C, the bending shape of ACF-type specimens was flat, it was determined that the temperature of the reference condition was set at 125 °C above T_g of ACF in the bithermal test. Therefore, the sectioned specimens were attached to the specimen grating at 125 °C. The frequency of the specimen grating was 1200 lines/mm. The bithermal test results at room temperature are shown in Fig. 6. The resolution of the Moiré fringe image was 0.417 $\mu\text{m}/\text{fringe displacement}$.

The shear strain of the edge of the chip is important for the reliability of the ACF package, and was calculated using (3) from the Moiré fringe image. In order to obtain more accurate shear strain data, a phase-shifting method was applied by using a lead–zirconium–titanate stage (Fig. 7) [17]. Fig. 8 shows the

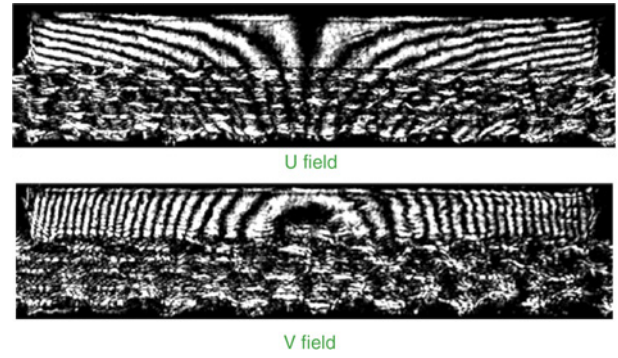


Fig. 6. Moiré fringe images of ACF-type specimen at 25 °C.

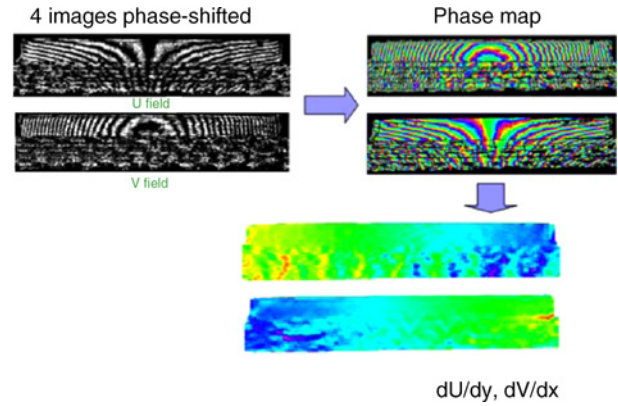


Fig. 7. Procedure of phase-shifting method.

shear strain distribution of each specimen. The S2 specimen had a small shear strain, but the S6 specimen had the largest shear strain. These results are shown in Fig. 9

$$\varepsilon_x = \frac{\partial U}{\partial x} = \frac{1}{f} \left(\frac{\partial N_x}{\partial x} \right) = \frac{1}{f} \left(\frac{\Delta N_x}{\Delta x} \right) \quad (1)$$

$$\varepsilon_y = \frac{\partial V}{\partial y} = \frac{1}{f} \left(\frac{\partial N_y}{\partial y} \right) = \frac{1}{f} \left(\frac{\Delta N_y}{\Delta y} \right) \quad (2)$$

$$\gamma_{xy} = \frac{\partial U}{\partial y} + \frac{\partial V}{\partial x} = \frac{1}{f} \left(\frac{\partial N_x}{\partial y} + \frac{\partial N_y}{\partial x} \right) = \frac{1}{f} \left(\frac{\Delta N_x}{\Delta y} + \frac{\Delta N_y}{\Delta x} \right) \quad (3)$$

Fig. 9 shows the relation of the shear strain and the thermal fatigue life. Application of moderate geometric shape was shown to be a powerful method for reducing the shear strain. The fillet at the edge of the chip was shown to be useful for increasing the thermal fatigue life. Consequently, low shear strain is shown to improve the reliability of the interconnection layer.

In order to predict the thermal fatigue life of the ACF-type package, a new damage model that considers the geometric shape and the fillet of the ACF-type package was developed. Equation (4) shows the thermal fatigue damage of one cycle at the edge of the chip

$$\Delta W = \tau \left(\frac{dw}{dT} \right) = (G\gamma) \left(\frac{dw}{dT} \right) \quad (4)$$

where G is shear modulus and γ is shear strain.

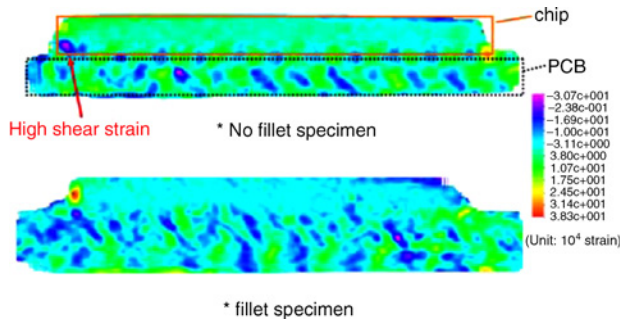


Fig. 8. Shear strain distributions of ACF-type specimens at 25 °C.

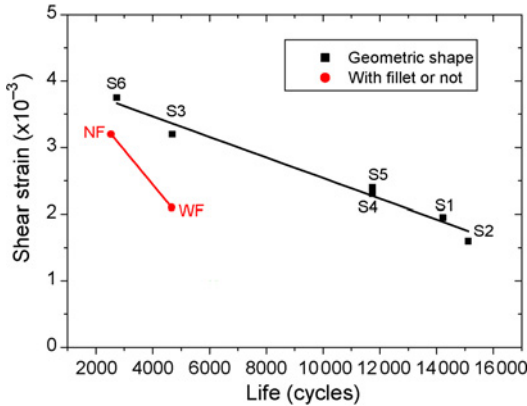


Fig. 9. Relations between thermal life and shear strain.

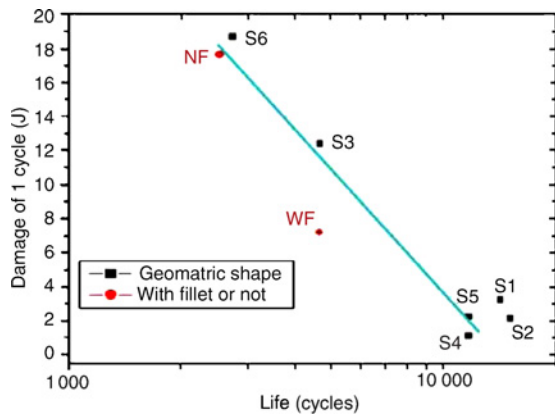


Fig. 10. Relations between thermal life and damage.

The thermal cycle damage of the polymeric resin attributed to gradual delamination growth at the chip and adhesive film interface induced by CTE mismatch driven shear. This delamination decreases the warpage of the chip. dw/dT denotes the warpage change of the chip during one thermal cycle. dw/dT is measured by Twyman–Green interferometry and takes into account the conditions of the geometric shape and the fillet. Fig. 10 shows the relation between the thermal fatigue damage per cycle and the package lifetime.

IV. HUMIDITY TESTS

Hygroscopic swelling assisted by loss of adhesion strength upon moisture absorption is responsible for moisture-induced

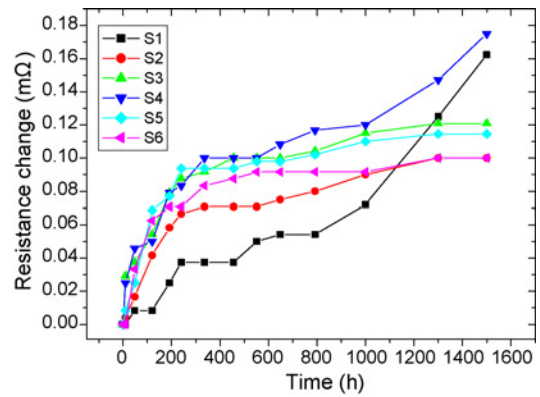


Fig. 11. Change of resistance in 85 °C/85% environment.

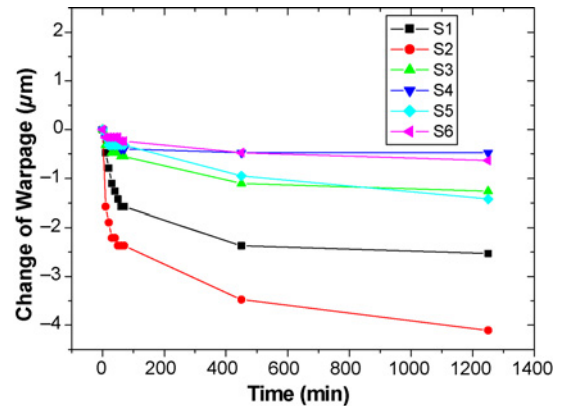


Fig. 12. Change of warpage in 85 °C/85% environment.

failure in the adhesive flip-chip interconnects. The diffusion of the water molecules into the space in the polymer chain causes swelling deformations. The polymer materials on the electronic package have different humidity properties from other materials in packages. The mismatch in CME between the adhesive and other components in the package induces hygroscopic swelling stress. Thus, understanding of the complicated hygroscopic swelling deformations is important to design adhesive-type packages [18].

Humidity tests of the ACF-type specimens were performed in a humidity chamber. The humidity test conditions were 85 °C/85%. Fig. 11 shows the change in resistance of the ACF package specimens.

The ACF and the PCB of the ACF package specimens were polymer materials. These polymer materials are swelled by absorbing water. At room temperature, the bending warpage decreased by the swelling deformation of the PCB, but peeling stress at the edge of the chip increased gradually. In order to shed light on these phenomena, experiments using Twyman–Green interferometry were performed. After drying ACF package specimens at 100 °C for 24 h, the warpage of the specimens in a 85 °C/85% humidity chamber was measured by Twyman–Green interferometry. Fig. 12 shows the warpage results. The warpage of the chip side decreased considerably. The total warpage of S2 specimen decrease was about 4 μm. This value is similar to the value

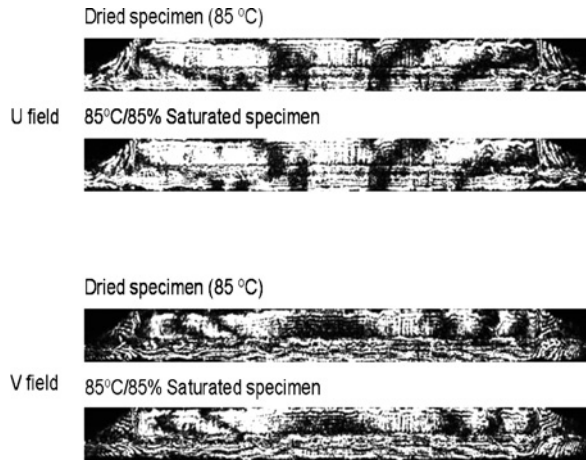


Fig. 13. Change of Moiré fringe patterns of S4 specimen induced by moisture.

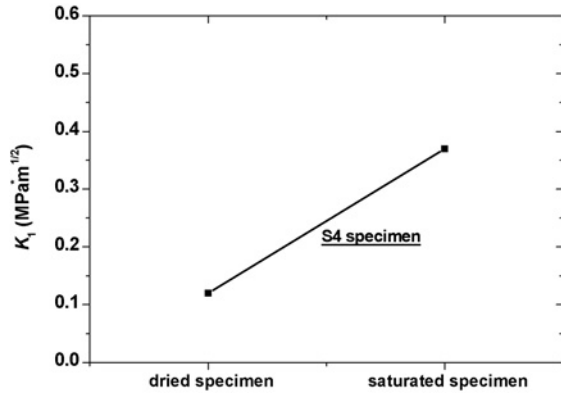


Fig. 14. Change of K_1 of S4 specimen during humidity tests.

obtained by increasing the temperature from room temperature to 75 °C. At high temperature, the amount of diffusion increases dramatically. After the polymer materials are fully saturated by moisture, the bonding strength of ACF decreases slowly.

The hygrothermal behavior of the ACF-type package is complicated. The ACF and the PCB of the ACF package specimens have the different humidity properties. The ACF layer showed larger hygro-swelling deformations than PCB in the ACF package specimens, and consequently a loss of adhesion strength occurred by moisture induced swelling. The ACF package specimens fully saturated by moisture showed large peeling stress at the edge of the chip. In order to elucidate these phenomena, experiments using Moiré interferometry were performed. After drying ACF package specimens at 100 °C for 24h, the strain distributions of the specimens in a 85 °C/85% humidity chamber after 1 week were measured by Moiré interferometry (Fig. 13). From the Moiré fringe results, we can calculate the stress intensity factor K by (5) [19], [20]. Since the specimens fully saturated by moisture showed large peeling stress at the edge of the chip, it was determined that these specimens had a larger K_1 than the dried specimens. Fig. 14 shows the K_1 result of S4 specimen

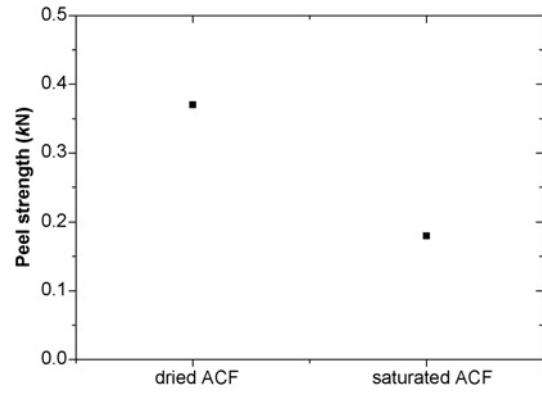


Fig. 15. Change of Peel strength of ACF.

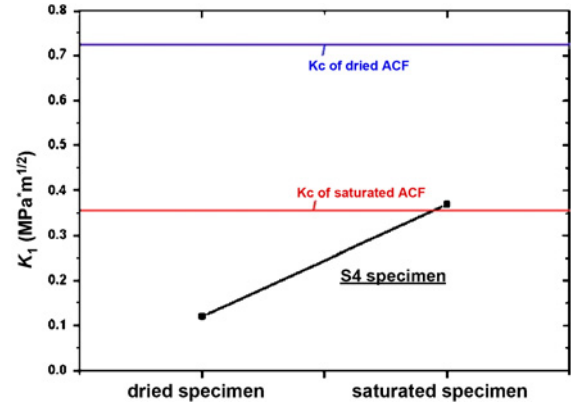


Fig. 16. Relation between stress intensity factor K of S4 specimen and the critical fracture toughness K_c .

$$K_1 = \frac{\{A \cos [\varepsilon \ln (\frac{r}{L})] + B \sin [\varepsilon \ln (\frac{r}{L})]\}}{D}$$

$$K_2 = \frac{\{B \cos [\varepsilon \ln (\frac{r}{L})] - A \sin [\varepsilon \ln (\frac{r}{L})]\}}{D} \quad (5)$$

where

$$A = \delta_y - 2\varepsilon\delta_x$$

$$B = \delta_x + 2\varepsilon\delta_y$$

$$D = \frac{8}{E^* \cosh(\pi\varepsilon)} \sqrt{\frac{r}{2\pi}} \quad (6)$$

In order to determine the loss of adhesion strength upon moisture absorption, a 90° peel strength test was performed [21]. Fig. 15 shows the strength results of a moisture saturated ACF specimen and a dried specimen. From these results, the critical fracture toughness K_c was calculated by (7) [20], [22]. G_c value was obtained by finite element analysis method. Fig. 16 shows the relations between the stress intensity factor K of S4 ACF specimen and the critical fracture toughness K_c . The dried ACF specimens had a lower K value than the K_c of the dried ACF interface. However, the moisture saturated ACF specimens had a similar K value with K_c of the saturated ACF interface.

$$|K_c|^2 = \frac{16 \cosh^2(\pi\varepsilon) G_c}{c_1 + c_2} \quad (7)$$

where

$$c_1 = \frac{\kappa_1 + 1}{\mu_1}, \quad c_2 = \frac{\kappa_2 + 1}{\mu_2} \quad (8)$$

where μ is shear modulus and $\kappa_i = 3 - 4\nu_i$ for plane strain.

V. CONCLUSION

In this paper, the hygrothermal behavior of an ACF-type package was evaluated. A primary factor of the ACF package failure is delamination between the chip and the adhesive at the edge of the chip. This delamination is mainly affected by the shear strain at the edge of the chip. Application of moderate geometric shape condition was shown to be a very powerful means for reducing the shear strain. Consequently, low shear strain was shown to improve the reliability of the interconnection layer. In order to predict the thermal fatigue life of the ACF-type package, a new damage model that considers the geometric shape and the fillet of the ACF-type package is proposed.

The polymer materials of ACF-type packages are swelled by absorbing the humidity. Mismatch in the CME between the adhesive and other components in the package induces hygroscopic swelling stress. The specimens fully saturated by moisture showed large peeling stress at the edge of the chip. Therefore, these specimens had a larger K_1 than the dried specimens.

In the research of the effect of moisture, it is concluded that hygroscopic swelling assisted by loss of adhesion strength upon moisture absorption is responsible for moisture-induced failures in these adhesive flip-chip interconnects.

REFERENCES

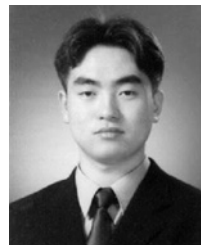
- [1] A. M. Lyons, E. E. Hall, Y.-H. Wong, G. Adams, "A new approach to using anisotropically conductive adhesives for flip-chip assembly," *IEEE Trans. Compon. Packag. Manuf. Technol. A*, vol. 19, no. 1, pp. 5–11, Mar. 1996.
- [2] J. S. Rasul, "Chip on paper technology utilizing anisotropically conductive adhesive for smart label applications," *Microelectron. Reliab.*, vol. 44, no. 1, pp. 135–140, 2004.
- [3] B. Han and P. Kunthong, "Micro-mechanical deformation analysis of surface laminar circuit in organic flip-chip package: An experimental study," *J. Electron. Packag.*, vol. 122, no. 4, pp. 294–300, 2000.
- [4] X. Huimin, C. G. Boay, A. Asundi, J. Yu, L. Yunguang, B. K. A. Ngoi, and Z. Zhaowei, "Thermal deformation measurement of electronic package using advanced Moiré methods," in *Proc. 3rd Electron. Packag. Technol. Conf.*, 2000, pp. 163–168.
- [5] M. R. Miller, I. Mohammed, and P. S. Ho, "Quantitative strain analysis of flip-chip electronic packages using phase-shifting Moiré interferometry," *Optics Lasers Eng.*, vol. 36, no. 2, pp. 127–139, 2001.
- [6] G. Wang, J.-H. Zhao, M. Ding, and P. S. Ho, "Thermal deformation analysis on flip-chip packages using high resolution Moiré interferometry," in *Proc. 18th Intersoc. Conf. Thermal Thermomech. Phenom. Electron. Syst.*, 2002, pp. 869–875.
- [7] D. Post, B. Han, and P. Ifju, *High Sensitivity Moiré*. New York: Springer-Verlag, 1994, p. 118.
- [8] A. F. Bastawros, A. S. Voloshin, and P. Rodogoveski, "Determination of thermally induced deformations in electronic packages by Moiré interferometry," in *Proc. 39th Electron. Compon. Technol. Conf. (ECTC)*, 1989, pp. 864–868.
- [9] B. Han and Y. Guo, "Determination of an effective coefficient of thermal expansion of electronic packaging components: A whole-field approach," *IEEE Trans. Compon., Packag., Manufact. Technol. A*, vol. 19, no. 2, pp. 240–247, Jun. 1996.

- [10] S. Liu, J. Zhu, D. Zou, and J. Benson, "Study of delaminated plastic packages by high temperature Moiré and finite element method," *IEEE Trans. Compon., Packag., Manufact. Technol. A*, vol. 20, no. 4, pp. 505–512, Dec. 1997.
- [11] Y. Guo and S. Liu, "Development in optical methods for reliability analysis in electronic packaging applications," *Am. Soc. Mech. Eng. J. Electron. Packag.*, vol. 120, no. 2, pp. 186–193, 1998.
- [12] B. Han, Y. Guo, C. K. Lim, and D. Caletka, "Verification of numerical models used in microelectronics packaging design by interferometric displacement measurement methods," *Am. Soc. Mech. Eng. J. Electron. Packag.*, vol. 118, no. 3, pp. 157–163, Sep. 1996.
- [13] L. L. Mercado, "Failure mechanism study of anisotropic conductive film (ACF) packages," *IEEE Trans. Compon. Packag. Technol.*, vol. 26, no. 3, pp. 509–516, Sep. 2003.
- [14] W. D. Driel, G. Q. Zhang, J. H. J. Janssen, L. J. Ernst, F. Su, K. S. Chian, and S. Yi, "Prediction and verification of process induced warpage of electronic packages," *Microelectron. Reliab.*, vol. 43, no. 5, pp. 765–774, May 2003.
- [15] K. Verma, S. B. Park, and B. Han, "On the design parameters of flip-chip PBGA package assembly for optimum solder ball reliability," *IEEE Trans. Compon. Packag. Technol.*, vol. 24, no. 2, pp. 300–307, Jun. 2001.
- [16] W. Zhang, D. Wu, B. Su, S. A. Hareb, Y. C. Lee, B. P. Masterson, "The effect of underfill epoxy on warpage in flip-chip assemblies," *IEEE Trans. Compon., Packag., Manufact. Technol. A*, vol. 21, no. 2, pp. 323–329, Jun. 1998.
- [17] S. Y. Yang and S. B. Lee, "Developing phase-shifting micro-Moiré interferometry using phase shifter with rough resolution and by shifting specimen grating," in *Proc. Electron. Mater. Packag.*, Jeju, Korea, Nov. 2001, pp. 399–403.
- [18] P. Seungbae, "Predictive model for optimized design parameters in flip-chip packages and assemblies," *IEEE Trans. Compon. Packag. Technol.*, vol. 30, no. 2, pp. 294–301, Jun. 2007.
- [19] X. Q. Shi, "Effect of hygrothermal aging on interfacial reliability of silicon/underfill/FR-4 assembly," *IEEE Trans. Compon. Packag. Technol.*, vol. 31, no. 1, pp. 94–103, Mar. 2008.
- [20] X. Q. Shi, "Determination of fracture toughness of underfill/chip interface with digital image speckle correlation technique," *IEEE Trans. Compon. Packag. Technol.*, vol. 30, no. 1, pp. 101–109, Mar. 2007.
- [21] M. J. Yim and K. W. Paik, "The contact resistance and reliability of anisotropically conductive film (ACF)," *IEEE Trans. Adv. Packag.*, vol. 22, no. 2, pp. 166–173, May 1999.
- [22] X. J. Fan, H. B. Wang, and T. B. Lim, "Investigation of the underfill delamination and cracking for flip-chip module during thermal cyclic loading," *IEEE Trans. Compon., Packag., Manufact. Technol.*, vol. 24, no. 1, pp. 84–91, Mar. 2001.



Jin-Hyoung Park received the B.S., M.S., and Ph.D. degrees in mechanical engineering from the Department of Mechanical Engineering, Korea Advanced Institute of Science and Technology (KAIST), Daejeon, in 2003, 2005, and 2009, respectively.

His research interests include reliability evaluation for flip-chip electronic packaging using optical measurement techniques and development of in-plane micro Moiré technique using the phase shifting method.



Kyung-Woon Jang received the B.S., M.S., and Ph.D. degrees in materials science and engineering from Korea Advanced Institute of Science and Technology (KAIST), Daejeon, in 2001, 2003, and 2008, respectively.

Since graduation he has been a Senior Engineer with the Mechatronics and Manufacturing Technology Center, Samsung Electronics, Suwon, Korea. His job applications are interconnection material and process development for advanced packaging and surface mount technology. His research interests

include developing anisotropic conductive adhesives (ACAs), reliability evaluation of flip chip packages using ACAs, and material development of epoxy/ceramic composite paste for embedded capacitors during the degree period.

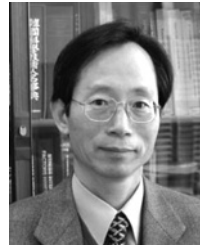


Kyung-Wook Paik received the Ph.D. degree from the Department of Materials Science and Engineering, Cornell University, Ithaca, NY, in 1981 and 1989, respectively.

From 1982 to 1985, he was with the Korea Advanced Institute of Science and Technology (KAIST), Seoul, as a Research Scientist, and was responsible for various materials developments, such as gold bonding wires and non-ferrous alloys. From 1989 to 1995, he was a Senior Technical Staff with the General Electric (GE) Corporate Research and

Development, Niskayuna, NY, where he was involved with the research and development of materials and processes of GE high density interconnect multichip module technology and power I/C packaging. Since 1995, he has been a Professor with the Department of Materials Science and Engineering, KAIST. In his Nano-Packaging and Interconnect Laboratory, he is currently working in the areas of flip chip bumping and assembly, adhesives flip chip, embedded capacitors, and display packaging technologies.

Dr. Paik has been a member of the IEEE Components, Packaging and Manufacturing Technology Society, the International Microelectronics and Packaging Society, and SEMI. He is also actively involved in different international electronic packaging conferences as an organizer, technical committee, international liaison, and chairs.



Soon-Bok Lee received the Ph.D. degree from the Department of Mechanical Engineering, Stanford University, Stanford, CA, in 1980.

He is currently a Professor with the Department of Mechanical Engineering, Korea Advanced Institute of Science and Technology (KAIST), Daejeon. His current research interests include reliability in electronics packaging, fatigue, and fracture mechanics. He is the author of *Korea's Electronics Industry* (CALCE EPSC Press, 2004). He has been actively involved in the national reliability enhancement program as a Chairman and Committee Member of the National Reliability

Counsel for Parts and Materials with the Ministry of Knowledge Economy.

Dr. Lee has organized the 3rd International Symposium on Electronics Materials and Packaging in 2001 (EMAP 2001) and the 5th International Conference on Experimental Mechanics (ICEM2006) as a General Chairman. He served as a Vice President of the Korea Reliability Society and also as the President of the Reliability Division with the Korea Society of Mechanical Engineers (KSME). He is a Member of KSME, KORAS, the American Society of Mechanical Engineers, IEEE, and the Society for Experimental Mechanics.